

Removing Powerline Interference Noise from Electrocardiogram (ECG) Signal

Ibrahem Soliman Al Sadi ^{1*}  , Sirajaldeen Alfthi ¹  

¹Department of Electrical and Electronic Engineering, Engineering Faculty, Wadi Alshatti University, Brack, Libya

ARTICLE HISTORY

Received 23 April 2025
Revised 19 June 2025
Accepted 25 June 2025
Online 29 June 2025

KEYWORDS

Electrocardiogram;
Powerline Interference;
Biorthogonal;
Symlets;
Signal-To-Noise Ratio (SNR);
Signal Correlation Value (SCV).

ABSTRACT

The electrocardiogram (ECG) is regarded as an essential diagnostic tool, as it serves as a representation of the cardiac electrical activity and is extensively employed in the diagnosis of cardiovascular diseases, as well as in assessing the overall health of the heart. ECG signals yield critical insights into the functional condition of the heart and its associated parameters; however, these signals are frequently vulnerable to distortion caused by various types of noise. Such noise includes powerline interference, baseline wandering, electromyographic noise (EMG noise), and artifacts resulting from electrode movement. Powerline interference is characterized by a 50 Hz frequency component, and its amplitude typically constitutes 50% of the peak-to-peak amplitude of the ECG signal. This interference predominantly arises from electromagnetic disturbances associated with power lines. The objective of this study is to process the ECG signal utilizing MATLAB. We employed a Notch filter for the initial preprocessing of the signal and applied two families of wavelets, namely Symlets and Biorthogonal wavelets, to mitigate the impact of powerline interference on the ECG signal. Subsequently, we compared the efficacy of these wavelet families in the signal processing framework by evaluating the Signal-to-Noise Ratio (SNR) and the Signal Correlation Value (SCV). The findings demonstrated that the Biorthogonal wavelet family outperformed the others, as the application of the Biorthogonal wavelet 2.4 resulted in a Signal-to-Noise Ratio of SNR=20.2553 dB and a Signal Correlation Value of SCV=0.9956.

إزالة تداخل خطوط الطاقة من إشارة تخطيط القلب (ECG)

إبراهيم سليمان الساعدي^{1*}، سراج الدين الفتحي¹

الكلمات المفتاحية	الملخص
تخطيط كهربية القلب تداخل خطوط الطاقة التعامد الحيوي نسبة الإشارة إلى الضوضاء (SNR) قيمة ارتباط الإشارة (SCV).	يُعد تخطيط كهربية القلب (ECG) أداة تشخيصية أساسية، إذ يُمثل النشاط الكهربائي للقلب، ويُستخدم على نطاق واسع في تشخيص أمراض القلب والأوعية الدموية، وكذلك في تقييم الصحة العامة للقلب. تُقدم إشارات تخطيط كهربية القلب رؤى بالغة الأهمية حول الحالة الوظيفية للقلب والمعلومات المرتبطة به؛ ومع ذلك، غالبًا ما تكون هذه الإشارات عرضة للتشويه الناتج عن أنواع مختلفة من الضوضاء. تشمل هذه الضوضاء تداخل خطوط الطاقة، وتجوّال خط الأساس، وضوضاء تخطيط كهربية القلب (ضوضاء تخطيط كهربية القلب)، والتشوهات الناتجة عن حركة الأقطاب الكهربائية. يتميز تداخل خطوط الطاقة بمكون تردد 50 هرتز، وتشكل سعته عادةً 50% من سعة إشارة تخطيط كهربية القلب من الذروة إلى الذروة. ينشأ هذا التداخل في الغالب من الاضطرابات الكهرومغناطيسية المرتبطة بخطوط الطاقة. الهدف من هذه الورقة هو معالجة إشارة تخطيط كهربية القلب باستخدام MATLAB. تم استخدام مرشح نوتش للمعالجة الأولية للإشارة، وطبقنا عائلتين من الموجات، وهما الموجات المتماثلة والموجات المتعامدة بيولوجيًا، لتخفيف تأثير تداخل خطوط الطاقة على إشارة تخطيط القلب. بعد ذلك، قارنا فعالية هاتين العائلتين في إطار معالجة الإشارة من خلال تقييم نسبة الإشارة إلى الضوضاء (SNR) وقيمة ارتباط الإشارة (SCV). أظهرت النتائج تفوق عائلة الموجات المتعامدة بيولوجيًا على غيرها، حيث أدى تطبيق الموجة المتعامدة بيولوجيًا 2.4 إلى نسبة إشارة إلى ضوضاء بلغت 20.2553 ديسيبل، وقيمة ارتباط الإشارة بلغت 0.9956 ديسيبل.

Introduction

An electrocardiogram (ECG) represents a documented manifestation of the electrical activity of the heart, serving as a prevalent diagnostic tool for heart disease. ECG signals yield critical insights regarding the operational conditions of the heart and the circulatory system. The frequency spectrum of an ECG signal typically spans from 0.05 to 100 Hz, with a dynamic range between 1 to 10 mV; given its nature as a weak non-static signal, ECG signals are frequently

compromised by various forms of noise, including power line interference, basic roaming (which encompasses electrode contact noise and movement), and electromyographic artifacts [1].

Power line interference constitutes a primary source of noise that often contaminates ECG signals, characterized by a 60 Hz (or 50 Hz in certain regions) sinusoidal waveform and its harmonics; this phenomenon is predominantly attributed to

*Corresponding author

electromagnetic interference generated by power lines, as well as electromagnetic fields emanating from proximate electrical apparatuses such as air conditioning units, elevators, and X-ray machines that exert considerable current draw on the power grid, consequently inducing 50 Hz signals within the input circuits of cardiac mapping devices. Additionally, the stray effects of alternating current fields resulting from cable loops and inadequate grounding of either the patient or the ECG apparatus further exacerbate this issue, wherein the presence of such extraneous interferences poses significant challenges in the accurate diagnosis of ECG readings. The mitigation of power line interference (PLI) from electrocardiogram (ECG) signals presents a significant challenge, as the frequency of power line noise resides within the overlapping frequency spectrum of both ECG and PLI signals [2]. Consequently, it is essential to implement appropriate signal processing techniques to proficiently eradicate PLI noise from ECG recordings. Moreover, the analysis of high-resolution ECG signals that are adversely affected by noise interference is of considerable importance, as the elimination of noise represents a fundamental challenge within the field of signal processing [3]. A range of diverse methodologies is utilized for the purpose of mitigating noise in electrocardiographic recordings.

In the study [4], eighteen ECG signals were extracted from the dominant noise using thirty-two discrete waveform transforms (DWTs). This method was used to evaluate the optimal performance in canceling power line interference. For comparison, the signals were also denoised using a conventional score filtering methodology, with the resulting data evaluated according to three performance metrics: signal-to-noise ratio (SNR), mean square error (MSE), and signal correlation value (SCV).

The subsequent study [5], sourced the reference ECG signal data from the MIT-BIH database. A multitude of filtering methodologies, including discrete wavelet transform (DWT), normalized least mean square (NLMS) filter, finite impulse response (FIR) filter, and infinite impulse response (IIR) filter, were employed in this study to mitigate the noise contaminating the compromised electrocardiogram (ECG) signal caused by (PLI). Subsequently, a comparative analysis of methodologies was conducted to identify the most efficacious strategy for mitigating distortion in a compromised ECG signal. The parameters employed for this evaluation encompassed Mean Squared Error (MSE), Mean Absolute Error (MAE), Signal-to-Noise Ratio (SNR), and Peak Signal-to-Noise Ratio (PSNR). An exemplary noise reduction algorithm demonstrates elevated values for SNR and PSNR, in conjunction with diminished values for MSE and MAE.

Electrocardiogram signal

Upon acquisition of the electrocardiographic (ECG) signal via an ECG apparatus, the amplitude of the signal, measured in millivolts, is graphically represented in conjunction with the temporal dynamics of the heart's electrical activity. Electrodes affixed to the dermal layer detect minuscule electrical variations, which adversely impact the normative ECG waveform and result in complications such as fibrillation, tachycardia, and inadequate perfusion in the coronary arteries. A Holter monitor may additionally be utilized to document the electrical phenomena associated with the cardiac muscle. An electrocardiogram, often denoted as ECG, constitutes a straightforward diagnostic procedure utilized to assess cardiac rhythm. Sensors or conductive

pathways are strategically positioned over the thorax, upper limbs, and lower limbs for a brief duration to capture the electrical signals emanating from the heart. The cardiologist meticulously scrutinizes these signals to ascertain any anomalies. An electrocardiogram is distinct from an echocardiogram, which represents a diagnostic examination focused on the structural and functional aspects of the heart. Normal electrical impulses facilitate the contraction of various segments of the heart, with alterations in these impulses serving as indicators of specific pathological conditions impacting cardiac function [6]. Figure 1 delineates the principal waves observable in the ECG output. There exist five primary waves manifested in the ECG results: "P, Q, R, S, T," sequentially. Each wave signifies a particular moment in the cardiac cycle during which electrical current traverses from the atria to the ventricles, while the intervals between the waves denote the duration required for the current to propagate from one point to another [7]. Figure (2) also illustrates the most critical segment of the ECG, namely the QRS complex, whose morphology and timing yield substantial statistics and insights regarding the heart's operational efficacy [2]. A conventional QRS detection algorithm typically encompasses two fundamental phases: preprocessing and resolution. The former exclusively entails a specific form of filtering [8], while the latter endeavors to identify QRS complexes within the ECG signal.

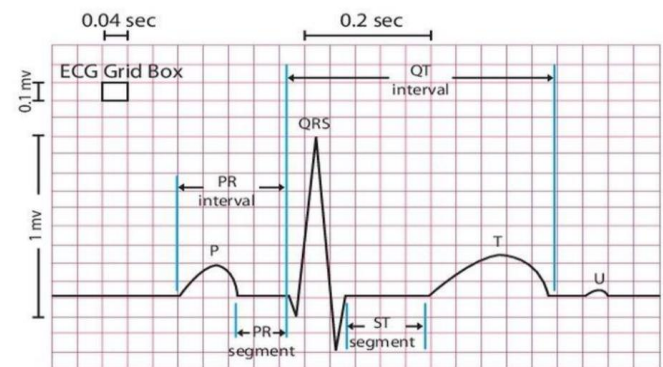


Fig. 1: ECG wave [9]

Power line interference noise

The power line operates at a frequency of 50 Hz, with the amplitude measured at 50% of the peak-to-peak electrocardiogram (ECG) amplitude [10]. Interference primarily arises from electromagnetic interference emanating from the power line, the electromagnetic fields (EMF) produced by nearby devices, the stray effects of alternating current (AC) fields due to cable loops, or through inadequate grounding of the patient or the ECG apparatus. Electrical devices generate 50 Hz signals within the input circuits. This phenomenon is particularly evident with ECG devices associated with air conditioning units, elevators, and X-ray machines that draw substantial current from the power line [11]. The electromagnetic fields produced by the power line represent a prevalent source of noise in the ECG, as well as in any other bioelectrical signals recorded from the body's surface. Such narrowband noise complicates the analysis and interpretation of the ECG, as it renders the identification of low-amplitude waveforms less reliable. Furthermore, it may introduce artifacts in the form of spurious waveforms. It is imperative to eliminate power line interference from ECG signals due to its complete disruption of low-frequency ECG waves, including the P wave and T wave [11]. Figure 2

shows the Powerline Interference Noise

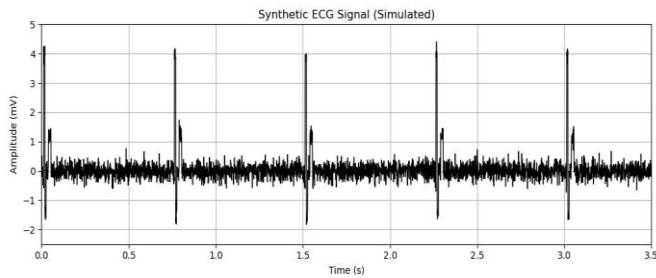


Fig. 2: Powerline Interference Noise [12]

Methodology

The methodology adopted in this study begins with the acquisition of an electrocardiogram (ECG) signal afflicted by powerline interference, a prevalent concern attributed to electromagnetic disturbances emanating from electrical apparatus or inadequate grounding practices. To mitigate this issue, an Infinite Impulse Response (IIR) Notch filter is initially implemented to eliminate the constant 50 Hz frequency component, ensuring minimal disruption to other segments of the signal. This filtering procedure diminishes the predominant noise, thereby establishing a more reliable basis for ensuing signal analysis. The resultant filtered signal is subsequently subjected to processing via the Discrete Wavelet Transform (DWT), utilizing two distinct families of wavelets: Symlets and Biorthogonal. Within the Biorthogonal domain, the wavelet coefficients are employed to reconstruct the signal, with the objective of achieving recovery with minimal distortion. Conversely, in the Symlets domain, the coefficients are utilized to derive performance metrics, including Signal-to-Noise Ratio (SNR), Mean Squared Error (MSE), and Signal Correlation Value (SCV). Upon the completion of evaluations across both branches, the resultant performance metrics of each wavelet family are meticulously compared to ascertain which yields superior noise attenuation. In light of these performance metrics, the wavelet type deemed most effective for mitigating powerline interference is identified. This culminates the methodology, which is predicated on wavelet-based signal processing methodologies to optimize ECG signal fidelity by reducing distortion as illustrated in Figure 3.

Discrete Wavelet Transform (DWT)

bands and distinct intensities by examining the signal for both detailed and approximate information, as elucidated in the subsequent two equations: [13].

$$c_{j+1}(k) = \sum_m L(z)(m - 2k) c_j \quad (1)$$

$$d_{j+1}(k) = \sum_m H(z)(m - 2k) c_j \quad (2)$$

The frequency of input signal is divided into frequency packets corresponding to the packet width through the utilization of the low and high-pass filters $L(Z)$ and $H(Z)$, respectively. The output generated by these filters exhibits half the frequency while retaining the sum of the samples from the input signal; furthermore, the combined outputs encapsulate the same frequency content as the input signal, thereby resulting in a data quantity that is effectively doubled [13], as illustrated in Fig. 4.

The original signal can be reconstructed utilizing the composition of bank filters. During the composition process, the signal is sampled in an upward vertical manner and subsequently processed through the $L(Z)$ and $H(Z)$ filters. The filters used in the synthesis process are derived from the

filters used in the analysis process, as they are combined with the outputs of the synthesis filters to reconstruct the signal $y(K)$ [13] as shown in Fig. 5.

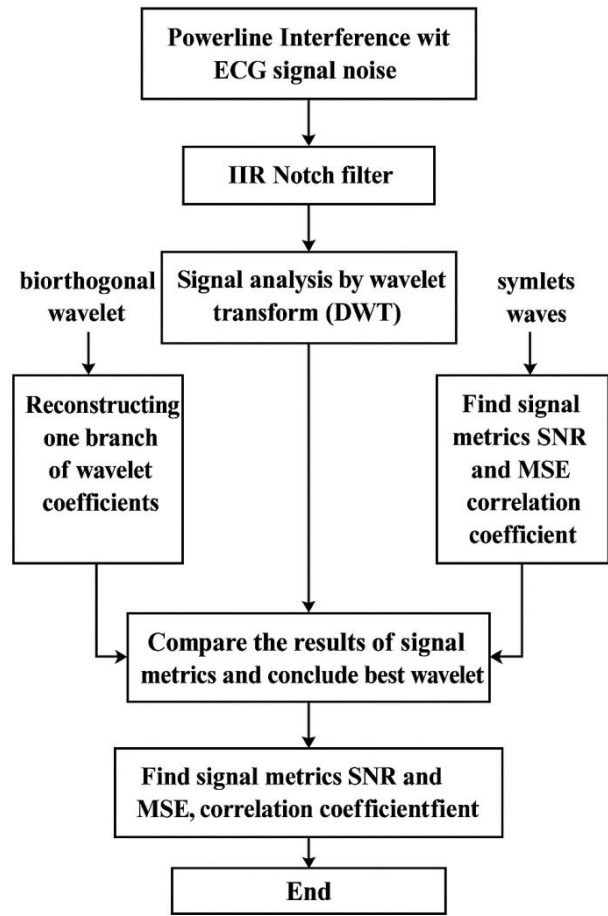


Fig.3: Flowchart of the methodology

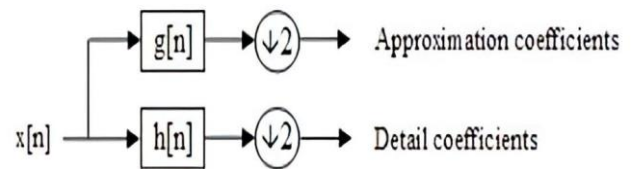


Fig. 4: Signal analysis using down sampling

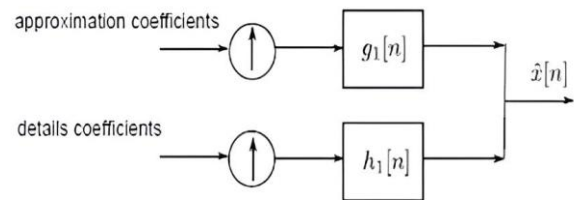


Fig. 5: Signal fitting using up sampling

The primary distinction between continuous wavelet transforms and discrete wavelet transforms lies in the capability to select a subset of the gradients and transitions requisite for processing, rather than executing the transformation across all gradients and transitions through temporal interruptions in the signal. This transformation yields a sufficient amount of information, with a reduction in computational time while concurrently preserving the fundamental information of the signal [14]. The wavelet

transform family encompasses various types, including Biorthogonal and Symlet, which are employed in this research as illustrated in Figure 6.

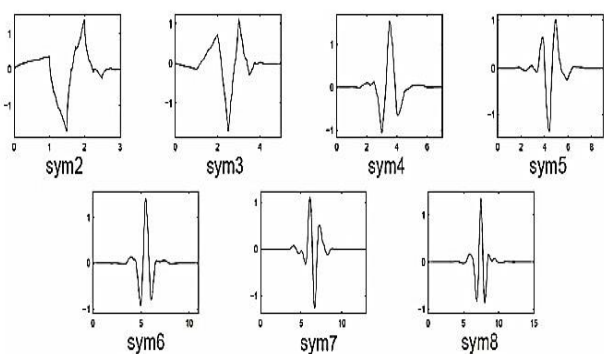


Fig. 6: Symlet family wavelets

Results and discussion

The objective of the filtering procedure is to diminish the noise levels within the signal, whilst concurrently ensuring that there is no alteration or distortion to the original waveform. The elimination of noise from the electrocardiogram (ECG) represents a critical challenge encountered by medical practitioners, as it is pivotal in the accurate diagnosis of cardiac disorders. In this paper, a simulation was performed to reduce the signal-to-noise ratio of the ECG. This section describes the main findings. The ECG signal, which exhibited power line interference noise, commonly referred to as Powerline Interference, was obtained as illustrated in Figure (7).

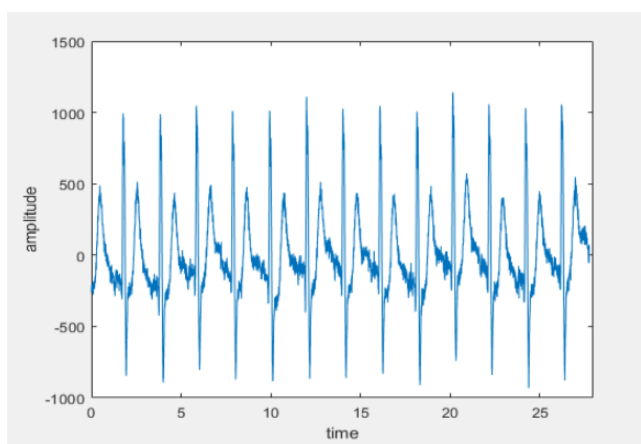


Fig. 7: ECG signal with noise (Powerline Interference)

To remove the noise from the ECG signal, an IIR notch filter was used as it is considered one of the best filters capable of producing a signal with higher contrast and clarity. Figure 8 shows the resulting signal after applying the IIR notch filter.

Use wavelet symlets

Figure (9) illustrates the transactions that were reconstructed subsequent to the application of wavelet analysis (sym2) to the signal produced by the notch filter depicted in Figure (8), wherein the discrete wavelet transform was employed on the resultant signal from the filter.

Figure (10) shows the transactions that were reconstructed using the sym4 wavelet and compare to Figure (9), which shows the reconstructed transactions in the case of sym2.

Figure (11) displays the transactions that were reconstructed employing the sym7 wavelet, in contrast to Figure (9), which

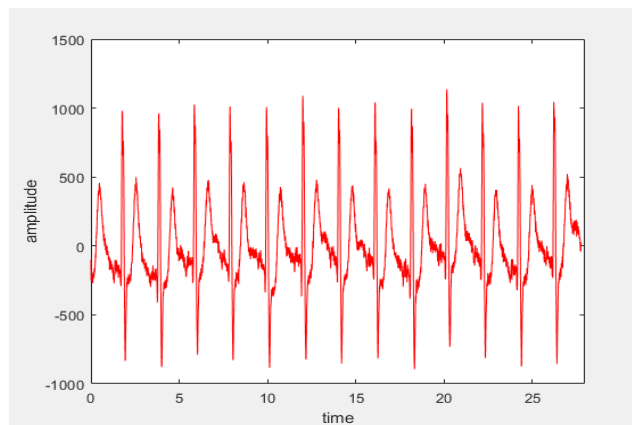


Fig. 8: The signal generated by applying the IIR Notch filter

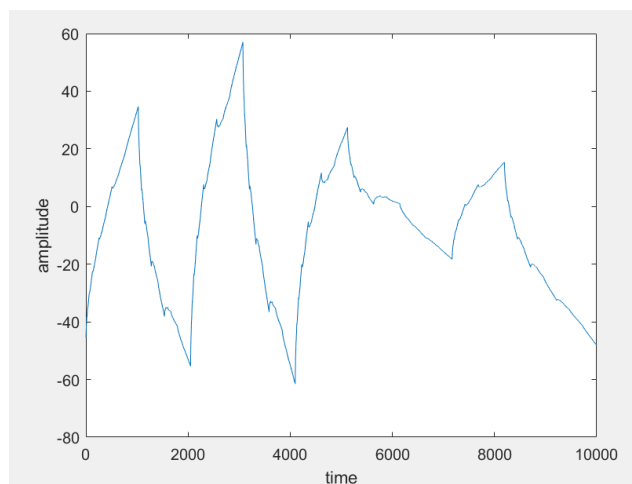


Fig. 9: The reconstructed transactions in the case of sym2

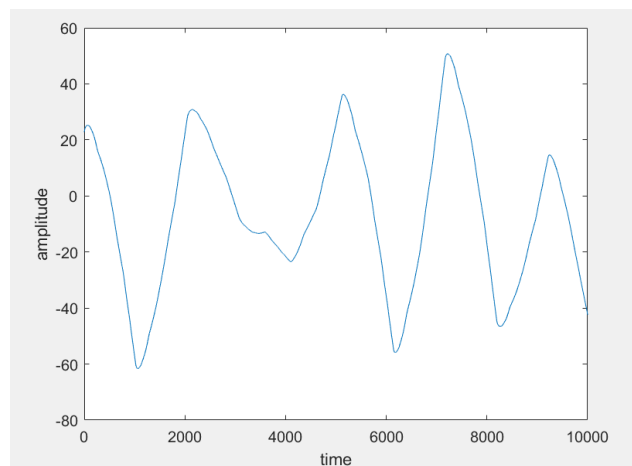


Fig. 10: The reconstructed transactions in the case of sym4

represents the reconstructed transactions associated with sym2, as well as Figure (10), which illustrates the reconstructed transactions relevant to sym4.

Due to the unique features of each wavelet, determining which one performed best in reconstructing the signal, as shown in the earlier figures (9), (10), and (11), can be quite difficult. Therefore, to facilitate comparison, we return to the signal metrics that clarify how effective the wavelet is in reconstructing the signal transactions. Additionally, the examination was carried out in four separate levels or stages to provide a more accurate time representation of the signal.

Figure (12) displays the original signal, which is influenced by noise from power line interference (PLI), alongside the signal that was filtered using the discrete wavelet transform (DWT) and then fitted to the transactions with the sym2 wavelet, which has proven successful in reconstructing the transactions after analysis.

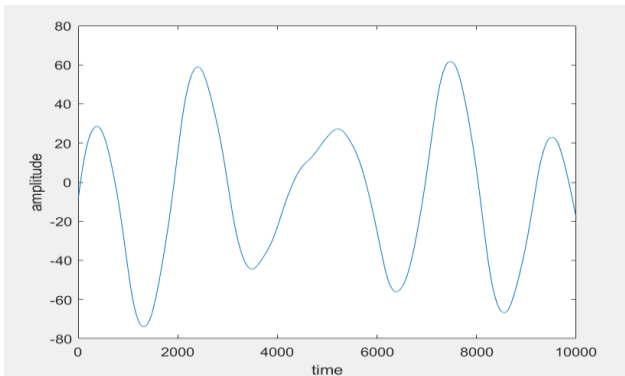


Fig. 11: The transactions that were reconstructed in the case of sym7

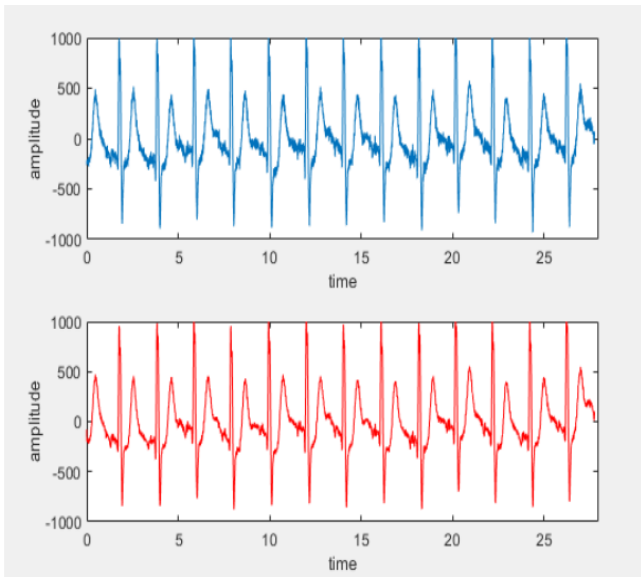


Fig. 12: The original signal filtered using the sym2 wavelet

Table 1: Comparison of wavelet symlets

Wavelet Type	SNR (dB)	(SCV)
Sym2	18.8864	0.99391
Sym3	17.7606	0.99374
Sym4	18.4228	0.99312
Sym5	18.7137	0.99364
Sym6	18.3944	0.99314
Sym7	16.7191	0.98975
Sym8	18.3718	0.99315

whereas: SNR refers to the ratio of the original signal to the noise present in the reconstructed signal. SCV denotes the correlation coefficient that exists between the original and the reconstructed signals.

This involves rebuilding the transactions after thorough examination.

• Use Biorthogonal wavelets

Figure (13) shows the coefficients that were restored after conducting wavelet analysis (bior2.4) on the signal obtained from the click filter illustrated in Figure (8), where the discrete wavelet transform was performed on the signal generated by the mentioned filter.

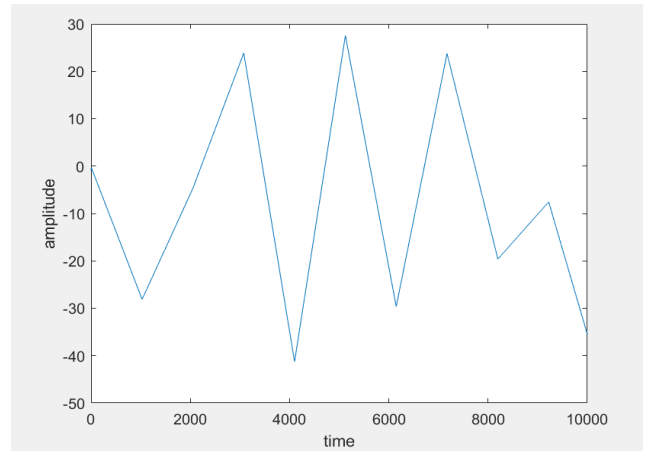


Fig. 13: The transactions that were reconstructed in the case of bior2.4

figure (14) presents the transactions that were reconstructed utilizing the bior1.5 wavelet, and is to be compared with Figure (13), which delineates the reconstructed transactions in the context of bior2.4.

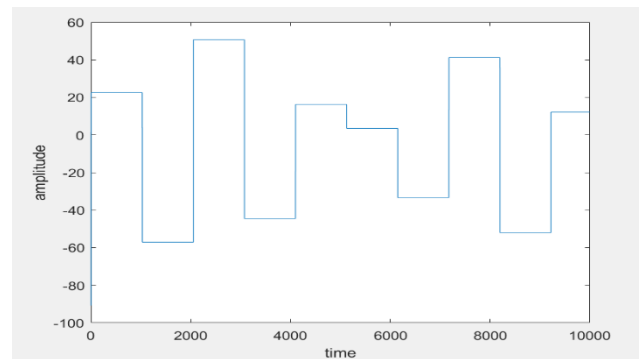


Fig. 14: The transactions that were reconstructed in the case of bior1.5

Figure (15) exhibits the transactions that were reconstructed through the implementation of the bior4.4 wavelet, and is to be contrasted with Figure (13), which illustrates the reconstructed transactions in the scenario of bior2.4, as well as Figure (14), which displays the reconstructed transactions in the instance of bior1.5.

Given the unique characteristics of each wavelet, it remains challenging to ascertain which wavelet exhibited superior performance in reconstructing the signal as evidenced by the preceding figures (13), (14), and (15). Consequently, in the evaluative process, we revert to the signal metrics, which elucidate the wavelet that performs optimally among the various wavelets in reconstructing the signal transactions. The analysis was conducted in four stages or levels to acquire the signal with enhanced temporal accuracy. Figure (16) portrays the original signal, which is contaminated with power line interference (PLI) noise, in conjunction with the signal that underwent filtration through the application of the discrete wavelet transform (DWT), and following the

adjustment of the coefficients employing the bior2.4 wavelet, which has demonstrated efficacy in reconstructing the coefficients post-analysis.

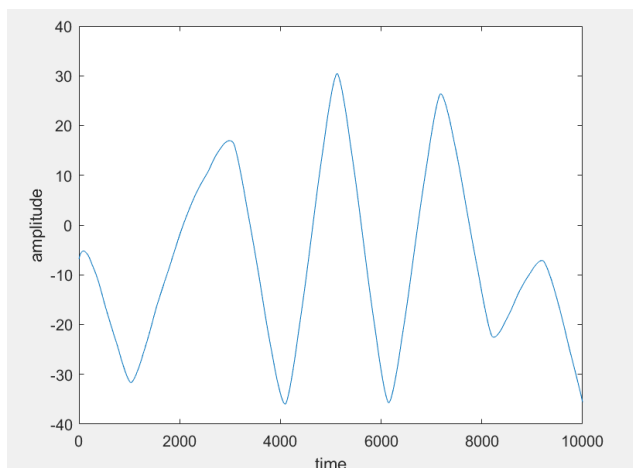


Fig. 15: The transactions that were reconstructed in the case of bior4.4

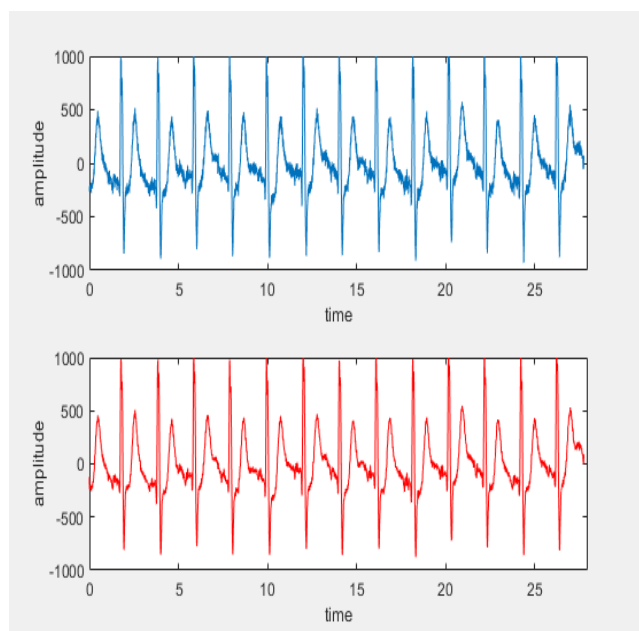


Fig. 16: The original signal and the filtered signal using the bior2.4 wavelet

Table 2: Comparison of Biorthogonal wavelets

Wavelet Type	SNR (dB)	(SCV)
Bior1.3	17.153	0.99056
Bior1.5	16.563	0.98991
Bior2.2	19.126	0.99413
Bior2.4	20.255	0.99561
Bior2.6	19.531	0.99418
Bior3.5	17.253	0.99079
Bior3.7	17.424	0.99076
Bior4.4	19.973	0.99532
Bior5.5	19.602	0.99491
Bior6.8	18.858	0.99393

• Compare symlets and biorthogonal wavelets

Table (3) delineates a comparative analysis of the outcomes

derived from the symlets and biorthogonal wavelet families. It is observed that the biorthogonal wavelet family, specifically the bior2.4 wavelet, exhibited superior performance in signal reconstruction.

Table 3: Comparison between the best results of the symlets and Biorthogonal wavelet families

Wavelet Type	SNR (dB)	(SCV)
Sym2	18.8864	0.9939
Sym4	18.4228	0.99312
Sym5	18.7137	0.99364
Bior2.4	20.255	0.99561
Bior4.4	19.973	0.99532
Bior5.5	19.602	0.99491

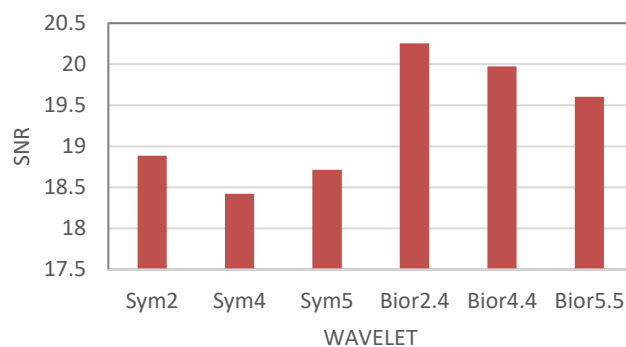


Fig. 17: The difference between the best results of wavelet families for (SNR)

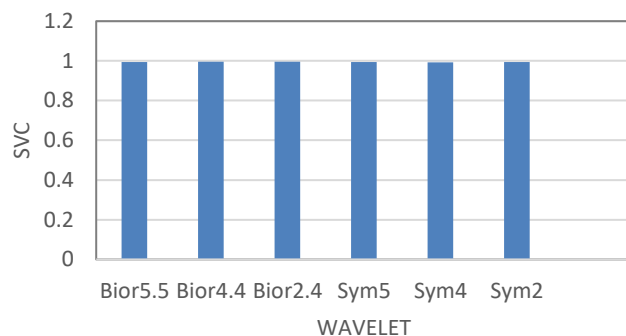


Fig. 18: The difference between the best results of wavelet families for (SCV)

Conclusions

In the realm of digital signal processing methodologies, the fidelity of the reconstructed signal emerges as a paramount consideration. The fidelity of the reconstructed signal must exhibit no discernible deviation from that of the original signal, and it is imperative that the signal is devoid of extraneous noise. This objective is achieved through the application of signal metrics, specifically the signal-to-noise ratio (SNR) and the signal correlation value (SCV).

1- The Symlets wavelet demonstrates significant utility in the analysis and reconstruction of the signal within the framework of the discrete wavelet transform. At the sym2 level, we achieved the optimal signal quality for the Symlets wavelet, wherein the SNR value was recorded at 18.8864 dB, accompanied by a signal correlation value of 0.9939.

2- The Biorthogonal wavelet exhibits commendable efficacy in the analysis and reconstruction of the signal when employed in the discrete wavelet transform. At the bior2.4

configuration, we achieved the highest signal quality for the Biorthogonal wavelet, where the SNR value was determined to be 20.2553 dB, alongside a signal correlation value of 0.9956.

3- In the present investigation, we undertook the processing of the signal and implemented a filtering procedure to mitigate the inherent noise through the discrete wavelet transform. Furthermore, we conducted a comparative analysis of two distinct families of discrete wavelet transforms and subsequently reconstructed the signal utilizing the discrete wavelet transform, which is recognized for its superior capabilities in both filtering and reconstructing the signal, demonstrating its efficacy particularly as the bior2.4 wavelet, which exhibited the most distinguished performance.

Recommendations

- 1- Dealing with heart rate signals associated with other types of noise, such as: EMG Noise and Electrode Motion Artifacts.
- 2- Use another type of filter in the pre-treatment process, such as: FIR Notch
- 3- Comparing other types of wavelet filters, such as: Haar wavelet, Daubechies, Coiflets, etc.
- 4- Use real heart rate signals by dealing with one of the centers specialized in heart rate signals.
- 5- Using compression as it removes unimportant or repetitive details to reduce the size of the signal.

Author Contributions: "All authors have made a substantial and direct intellectual contribution to the work and approved its publication."

Funding: "This research received no external funding."

Data Availability Statement: "No data were used to support this study".

Conflicts of Interest: "The authors declare that they have no conflict of interest".

References

- [1] S. M. Muhumed and M. I. Ibrahimy, "Noise reduction techniques in ECG signal," *Asian Journal of Electrical and Electronic Engineering*, vol. 3, no. 1, pp. 27–33, 2023. <https://doi.org/10.69955/ajoeee.2023.v3i1.43>
- [2] E. Ebrahimzadeh, M. Pooyan, S. Jahani, A. Bijar, and S. K. Setaredan, "ECG signals noise removal: Selection and optimization of the best adaptive filtering algorithm based on various algorithms comparison," *Biomedical Engineering: Applications, Basis and Communications*, vol. 27, no. 4, Art. 1550038, 2015, <https://doi.org/10.4015/S1016237215500386>.
- [3] R. Kher, "Signal processing techniques for removing noise from ECG signals," *Journal of Biomedical Engineering and Research*, vol. 3, no. 1, pp. 1–9, 2019, <https://doi.org/10.17303/jber.2019.3.101>.
- [4] J. Goodfellow, O. J. Escalona, V. Kodoth, and G. Manoharan, "Efficacy of DWT denoising in the removal of power line interference and the effect on morphological distortion of underlying atrial fibrillatory waves in AF-ECG," in *Proc. World Congress on Medical Physics and Biomedical Engineering (IFMBE Proc., vol. 51)*, Toronto, ON, Canada, pp. 1056–1059, 2015. https://doi.org/10.1007/978-3-319-19387-8_257.
- [5] S. Saxena, R. Jais, and M. Hota, "Removal of powerline interference from ECG signal using FIR, IIR, DWT and NLMS adaptive filter," in *Proc. 2019 International Conference on Communication and Signal Processing (ICCSPP)*, Chennai, India, pp. 12–16, 2019. <https://doi.org/10.1109/ICCSPP.2019.8698112>.
- [6] M. D'Aloia, A. Longo, and M. Rizzi, "Noisy ECG signal analysis for automatic peak detection," *Information*, vol. 10, no. 2, p. 35, 2019. <https://doi.org/10.3390/info10020035>.
- [7] P. Romero, L. Romaguera, C. Vázquez-Seisdedos, C. Costa, M. Costa, and J. Neto, "Baseline wander removal methods for ECG signals: A comparative study," *arXiv preprint arXiv:1807.11359*, 2019. <https://doi.org/10.48550/arXiv.1807.11359>.
- [8] R. Costa, T. Winkert, A. Manhães, and J. Teixeira, "QRS peaks, P and T waves identification in ECG," *Procedia Computer Science*, vol. 181, pp. 957–964, 2021. <https://doi.org/10.1016/j.procs.2021.01.252>.
- [9] O. Beya, M. Hittawe, N. Zegadi, E. Fauvet, and O. Lalignant, "Electrocardiogram signal analysing – delineation and localization of ECG component," in *Proceedings of the 9th International Joint Conference on Biomedical Engineering Systems and Technologies (BIOSTEC 2016) – BIOSIGNALS*, vol. 4, pp. 156–161, 2016. <https://doi.org/10.5220/0005684501560161>.
- [10] A. Velayudhan and S. Peter, "Noise analysis and different denoising techniques of ECG signal – A survey," in *Proc. Int. Conf. Emerging Trends in Engineering & Management (ICETEM)*, Kerala, India, pp. 40–44, 2016. <https://www.iosrjournals.org/iosr-jece/papers/ICETEM/Vol.%201%20Issue%201/ECE%2006-40-44.pdf>.
- [11] S. Saxena and M. Hota, "Removing power line interference from ECG signal using adaptive filter and notch filter," *IEEE Access*, vol. 7, pp. 150667–150676, 2019. <https://doi.org/10.1109/ACCESS.2019.2944027>.
- [12] H. Limaye and V. Deshmukh, "ECG noise sources and various noise removal techniques: A survey," *International Journal of Application or Innovation in Engineering & Management*, vol. 5, no. 2, pp. 86–92, 2016. <https://doi.org/10.2648/IJAEM.789.1630>.
- [13] Y. Al-Irham and A. Suliman, "Sound signal de-noising using wavelet transform," *Mosul University Journal*, vol. 9, pp. 143–157, Dec. 2019.
- [14] M. M. Helal, S. Saraya, and S. El-Taweel, "Lossless image compression using wavelet and vector quantization," *Mansoura Engineering Journal*, vol. 31, no. 3, pp. 8–17, 2006.